ROBERT J. FARRAUTO
LUCAS DORAZIO
C. H. BARTHOLOMEW

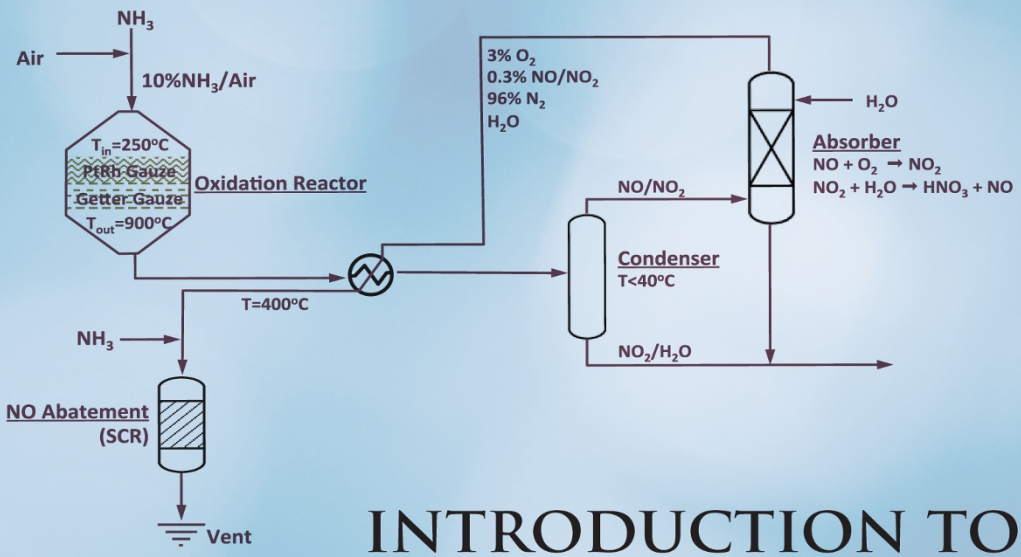

INTRODUCTION TO CATALYSIS AND INDUSTRIAL CATALYTIC PROCESSES

AIChE The Global Home of Chemical Engineers

WILEY

INTRODUCTION TO CATALYSIS AND INDUSTRIAL CATALYTIC PROCESSES

INTRODUCTION TO CATALYSIS AND INDUSTRIAL CATALYTIC PROCESSES

ROBERT J. FARRAUTO
Earth and Environmental Engineering Department
Columbia University
New York, New York

LUCAS DORAZIO
BASF Corporation
Iselin, New Jersey

C.H. BARTHOLOMEW
Department of Chemical Engineering
Brigham Young University
Provo, Utah

AIChE The Global Home of Chemical Engineers

WILEY

A joint publication of the American Institute of Chemical Engineers, Inc. and John Wiley & Sons, Inc.

Published by John Wiley & Sons, Inc., Hoboken, New Jersey.
Published simultaneously in Canada.

Library of Congress Cataloging-in-Publication Data:

Names: Farrauto, Robert J., 1941- author. | Dorazio, Lucas, author. |
Bartholomew, C. H., author.
Title: Introduction to catalysis and industrial catalytic processes / Robert
J. Farrauto, Lucas Dorazio, C. H. Bartholomew.
Description: Hoboken : John Wiley & Sons, Inc., 2016. | Includes index.
Identifiers: LCCN 2015042209 (print) | LCCN 2015044585 (ebook) | ISBN
9781118454602 (cloth) | ISBN 9781119089155 (pdf) | ISBN 9781119101673 (epub)
Subjects: LCSH: Catalysis.
Classification: LCC QD505 .F37 2016 (print) | LCC QD505 (ebook) | DDC
660/.2995–dc23
LC record available at http://lccn.loc.gov/2015042209

Printed in the United States of America.

10 9 8 7 6 5 4 3 2 1

To my wife Olga (Olechka) who has been a partner, friend, and critic over the precious years we have been together. She has provided love, understanding, focus, and a new vision to life. I thank my loving daughters, Jill Marie and Maryellen, and their husbands Glenn and Tom. I am fortunate to have inspiring grandchildren Nicky, Matt, Kevin, Jillian, Owen, and Brendan and stepdaughters Elena and Marina. I want to acknowledge my brother John (wife Noella) and sister Marianna (husband Ron) who have supported me emotionally through all of our years together. I am forever grateful to my parents who raised me as a proud Italian-American with a desire to help others.

Robert J. Farrauto

To my wife Cara, whose encouragement and support helped complete this project, and to my young children Lauren and Zach for their support and genuine interest in my career.

Lucas Dorazio

To my loving wife, friend, and critic, Karen, of over 49 years, who has supported me in all good things and forgiven my faults and mistakes; my 5 children and 10 grandchildren who have brought me mostly joy, been a constant source of fun and entertainment, and have given me understanding, support, love, excitement, inspiration, and challenges that have led to my growth; my loving, supportive brothers and sisters (all 7); and my dad and mom who taught me to love learning, life, and the Christian way. I especially dedicate this work (an offspring of our earlier book) to my son Charles who died unexpectedly on September 25, 2014 and who greatly touched and brightened the lives of his family, friends, and coworkers.

Calvin H. Bartholomew

CONTENTS

PREFACE **XV**

ACKNOWLEDGMENTS **XVII**

LIST OF FIGURES **XIX**

NOMENCLATURE **XXVII**

CHAPTER 1 *CATALYST FUNDAMENTALS OF INDUSTRIAL CATALYSIS* **1**

1.1 Introduction **1**
1.2 Catalyzed versus Noncatalyzed Reactions **1**
1.2.1 Example Reaction: Liquid-Phase Redox Reaction **2**
1.2.2 Example Reaction: Gas-Phase Oxidation Reaction **4**
1.3 Physical Structure of a Heterogeneous Catalyst **6**
1.3.1 Active Catalytic Species **7**
1.3.2 Chemical and Textural Promoters **7**
1.3.3 Carrier Materials **8**
1.3.4 Structure of the Catalyst and Catalytic Reactor **8**
1.4 Adsorption and Kinetically Controlled Models for Heterogeneous Catalysis **10**
1.4.1 Langmuir Isotherm **11**
1.4.2 Reaction Kinetic Models **13**
1.4.2.1 Langmuir–Hinshelwood Kinetics for CO Oxidation on Pt **14**
1.4.2.2 Mars–van Krevelen Kinetic Mechanism **17**
1.4.2.3 Eley–Rideal (E–R) Kinetic Mechanism **18**
1.4.2.4 Kinetic versus Empirical Rate Models **18**
1.5 Supported Catalysts: Dispersed Model **19**
1.5.1 Chemical and Physical Steps Occurring during Heterogeneous Catalysis **19**
1.5.2 Reactant Concentration Gradients within the Catalyzed Material **22**
1.5.3 The Rate-Limiting Step **22**
1.6 Selectivity **24**
1.6.1 Examples of Selectivity Calculations for Reactions with Multiple Products **25**
1.6.2 Carbon Balance **26**
1.6.3 Experimental Methods for Measuring Carbon Balance **27**
Questions **27**
Bibliography **29**

CHAPTER 2 *THE PREPARATION OF CATALYTIC MATERIALS* **31**

2.1 Introduction **31**
2.2 Carrier Materials **32**

2.2.1 Al_2O_3 32
2.2.2 SiO_2 34
2.2.3 TiO_2 34
2.2.4 Zeolites 35
2.2.5 Carbons 37
2.3 Incorporating the Active Material into the Carrier 37
2.3.1 Impregnation 37
2.3.2 Incipient Wetness or Capillary Impregnation 38
2.3.3 Electrostatic Adsorption 38
2.3.4 Ion Exchange 38
2.3.5 Fixing the Catalytic Species 39
2.3.6 Drying and Calcination 39
2.4 Forming the Final Shape of the Catalyst 40
2.4.1 Powders 40
2.4.1.1 Milling and Sieving 41
2.4.1.2 Spray Drying 42
2.4.2 Pellets, Pills, and Rings 43
2.4.3 Extrudates 43
2.4.4 Granules 44
2.4.5 Monoliths 44
2.5 Catalyst Physical Structure and Its Relationship to Performance 45
2.6 Nomenclature for Dispersed Catalysts 45
Questions 46
Bibliography 46

CHAPTER 3 *CATALYST CHARACTERIZATION* 48

3.1 Introduction 48
3.2 Physical Properties of Catalysts 49
3.2.1 Surface Area and Pore Size 49
3.2.1.1 Nitrogen Porosimetry 49
3.2.1.2 Pore Size by Mercury Intrusion 51
3.2.2 Particle Size Distribution of Particulate Catalyst 51
3.2.2.1 Particle Size Distribution 51
3.2.2.2 Mechanical Strength 53
3.2.3 Physical Properties of Environmental Washcoated Monolith Catalysts 54
3.2.3.1 Washcoat Thickness 54
3.2.3.2 Washcoat Adhesion 54
3.3 Chemical and Physical Morphology Structures of Catalytic Materials 54
3.3.1 Elemental Analysis 54
3.3.2 Thermal Gravimetric Analysis and Differential Thermal Analysis 55
3.3.3 The Morphology of Catalytic Materials by Scanning Electron Microscopy 56
3.3.4 Structural Analysis by X-Ray Diffraction 57
3.3.5 Structure and Morphology of Al_2O_3 Carriers 58
3.3.6 Dispersion or Crystallite Size of Catalytic Species 58
3.3.6.1 Chemisorption 58
3.3.6.2 Transmission Electron Microscopy 61
3.3.7 X-Ray Diffraction 62

3.3.8 Surface Composition of Catalysts by X-Ray Photoelectron Spectroscopy 62
3.3.9 The Bonding Environment of Metal Oxides by Nuclear Magnetic Resonance 64
3.4 Spectroscopy 65
Questions 66
Bibliography 67

CHAPTER 4 *REACTION RATE IN CATALYTIC REACTORS* 69

4.1 Introduction 69
4.2 Space Velocity, Space Time, and Residence Time 69
4.3 Definition of Reaction Rate 71
4.4 Rate of Surface Kinetics 72
4.4.1 Empirical Power Rate Expressions 72
4.4.2 Experimental Measurement of Empirical Kinetic Parameters 73
4.4.3 Accounting for Chemical Equilibrium in Empirical Rate Expression 77
4.4.4 Special Case for First-Order Isothermal Reaction 77
4.5 Rate of Bulk Mass Transfer 78
4.5.1 Overview of Bulk Mass Transfer Rate 78
4.5.2 Origin of Bulk Mass Transfer Rate Expression 79
4.6 Rate of Pore Diffusion 80
4.6.1 Overview of Pore Diffusion 80
4.6.2 Pore Diffusion Theory 81
4.7 Apparent Activation Energy and the Rate-Limiting Process 82
4.8 Reactor Bed Pressure Drop 83
4.9 Summary 84
Questions 84
Bibliography 87

CHAPTER 5 *CATALYST DEACTIVATION* 88

5.1 Introduction 88
5.2 Thermally Induced Deactivation 88
5.2.1 Sintering of the Catalytic Species 89
5.2.2 Sintering of Carrier 92
5.2.3 Catalytic Species–Carrier Interactions 95
5.3 Poisoning 96
5.3.1 Selective Poisoning 96
5.3.2 Nonselective Poisoning or Masking 97
5.4 Coke Formation and Catalyst Regeneration 99
Questions 101
Bibliography 103

CHAPTER 6 *GENERATING HYDROGEN AND SYNTHESIS GAS BY CATALYTIC HYDROCARBON STEAM REFORMING* 104

6.1 Introduction 104
6.1.1 Why Steam Reforming with Hydrocarbons? 104
6.2 Large-Scale Industrial Process for Hydrogen Generation 105
6.2.1 General Overview 105

6.2.2 Hydrodesulfurization **106**
6.2.3 Hydrogen via Steam Reforming and Partial Oxidation **106**
6.2.3.1 Steam Reforming **106**
6.2.3.2 Deactivation of Steam Reforming Catalyst **110**
6.2.3.3 Pre-reforming **111**
6.2.3.4 Partial Oxidation and Autothermal Reforming **111**
6.2.4 Water Gas Shift **112**
6.2.4.1 Deactivation of Water Gas Shift Catalyst **116**
6.2.5 Safety Considerations During Catalyst Removal **116**
6.2.6 Other CO Removal Methods **116**
6.2.6.1 Pressure Swing Absorption **116**
6.2.6.2 Methanation **117**
6.2.6.3 Preferential Oxidation of CO **117**
6.2.7 Hydrogen Generation for Ammonia Synthesis **119**
6.2.8 Hydrogen Generation for Methanol Synthesis **120**
6.2.9 Synthesis Gas for Fischer–Tropsch Synthesis **120**
6.3 Hydrogen Generation for Fuel Cells **121**
6.3.1 New Catalyst and Reactor Designs for the Hydrogen Economy **122**
6.3.2 Steam Reforming **123**
6.3.3 Water Gas Shift **124**
6.3.4 Preferential Oxidation **125**
6.3.5 Combustion **125**
6.3.6 Autothermal Reforming for Complicated Fuels **126**
6.3.7 Steam Reforming of Methanol: Portable Power Applications **126**
6.4 Summary **126**
Questions **127**
Bibliography **128**

CHAPTER 7 *AMMONIA, METHANOL, FISCHER–TROPSCH PRODUCTION* **129**

7.1 Ammonia Synthesis **129**
7.1.1 Thermodynamics **129**
7.1.2 Reaction Chemistry and Catalyst Design **130**
7.1.3 Process Design **132**
7.1.4 Catalyst Deactivation **134**
7.2 Methanol Synthesis **134**
7.2.1 Process Design **136**
7.2.1.1 Quench Reactor **136**
7.2.1.2 Staged Cooling Reactor **137**
7.2.1.3 Tube-Cooled Reactor **137**
7.2.1.4 Shell-Cooled Reactor **138**
7.2.2 Catalyst Deactivation **139**
7.3 Fischer–Tropsch Synthesis **140**
7.3.1 Process Design **142**
7.3.1.1 Bubble/Slurry-Phase Process **142**
7.3.1.2 Packed Bed Process **143**
7.3.1.3 Slurry/Loop Reactor (Synthol Process) **143**
7.3.2 Catalyst Deactivation **143**
Questions **144**
Bibliography **145**

CHAPTER 8 *SELECTIVE OXIDATIONS* **146**

8.1 Nitric Acid **146**
8.1.1 Reaction Chemistry and Catalyst Design **146**
8.1.1.1 The Importance of Catalyst Selectivity **147**
8.1.1.2 The PtRh Alloy Catalyst **147**
8.1.2 Nitric Acid Production Process **148**
8.1.3 Catalyst Deactivation **150**
8.2 Hydrogen Cyanide **151**
8.2.1 HCN Production Process **152**
8.2.2 Deactivation **152**
8.3 The Claus Process: Oxidation of H_2S **154**
8.3.1 Clause Process Description **154**
8.3.2 Catalyst Deactivation **155**
8.4 Sulfuric Acid **155**
8.4.1 Sulfuric Acid Production Process **155**
8.4.2 Catalyst Deactivation **158**
8.5 Ethylene Oxide **159**
8.5.1 Catalyst **159**
8.5.2 Catalyst Deactivation **160**
8.5.3 Ethylene Oxide Production Process **160**
8.6 Formaldehyde **160**
8.6.1 Low-Methanol Production Process **162**
8.6.1.1 Fe + Mo Catalyst **162**
8.6.2 High-Methanol Production Process **163**
8.6.2.1 Ag Catalyst **164**
8.7 Acrylic Acid **164**
8.7.1 Acrylic Acid Production Process **164**
8.7.2 Acrylic Acid Catalyst **165**
8.7.3 Catalyst Deactivation **166**
8.8 Maleic Anhydride **166**
8.8.1 Catalyst Deactivation **166**
8.9 Acrylonitrile **166**
8.9.1 Acrylonitrile Production Process **167**
8.9.2 Catalyst **168**
8.9.3 Deactivation **168**
Questions **168**
Bibliography **169**

CHAPTER 9 *HYDROGENATION, DEHYDROGENATION, AND ALKYLATION* **171**

9.1 Introduction **171**
9.2 Hydrogenation **171**
9.2.1 Hydrogenation in Stirred Tank Reactors **171**
9.2.2 Kinetics of a Slurry-Phase Hydrogenation Reaction **174**
9.2.3 Design Equation for the Continuous Stirred Tank Reactor **176**
9.3 Hydrogenation Reactions and Catalysts **177**
9.3.1 Hydrogenation of Vegetable Oils for Edible Food Products **177**
9.3.2 Hydrogenation of Functional Groups **180**
9.3.3 Biomass (Corn Husks) to a Polymer **183**

9.3.4 Comparing Base Metal and Precious Metal Catalysts **183**
9.4 Dehydrogenation **185**
9.5 Alkylation **187**
Questions **188**
Bibliography **189**

CHAPTER 10 *PETROLEUM PROCESSING* **190**

10.1 Crude Oil **190**
10.2 Distillation **191**
10.3 Hydrodemetalization and Hydrodesulfurization **193**
10.4 Hydrocarbon Cracking **197**
10.4.1 Fluid Catalytic Cracking **197**
10.4.2 Hydrocracking **200**
10.5 Naphtha Reforming **200**
Questions **202**
Bibliography **203**

CHAPTER 11 *HOMOGENEOUS CATALYSIS AND POLYMERIZATION CATALYSTS* **205**

11.1 Introduction to Homogeneous Catalysis **205**
11.2 Hydroformylation: Aldehydes from Olefins **206**
11.3 Carboxylation: Acetic Acid Production **208**
11.4 Enzymatic Catalysis **209**
11.5 Polyolefins **210**
11.5.1 Polyethylene **210**
11.5.2 Polypropylene **212**
Questions **213**
Bibliography **213**

CHAPTER 12 *CATALYTIC TREATMENT FROM STATIONARY SOURCES: HC, CO, NO_X, AND O_3* **215**

12.1 Introduction **215**
12.2 Catalytic Incineration of Hydrocarbons and Carbon Monoxide **216**
12.2.1 Monolith (Honeycomb) Reactors **218**
12.2.2 Catalyzed Monolith (Honeycomb) Structures **219**
12.2.3 Reactor Sizing **220**
12.2.4 Catalyst Deactivation **222**
12.2.5 Regeneration of Deactivated Catalysts **224**
12.3 Food Processing **225**
12.3.1 Catalyst Deactivation **226**
12.4 Nitrogen Oxide (NO_x) Reduction from Stationary Sources **226**
12.4.1 SCR Technology **227**
12.4.2 Ozone Abatement in Aircraft Cabin Air **229**
12.4.3 Deactivation **229**
12.5 CO_2 Reduction **230**
Questions **231**
Bibliography **233**

CHAPTER 13 *CATALYTIC ABATEMENT OF GASOLINE ENGINE EMISSIONS* **235**

13.1 Emissions and Regulations **235**
13.1.1 Origins of Emissions **235**
13.1.2 Regulations in the United States **236**
13.1.3 The Federal Test Procedure for the United States **238**
13.2 Catalytic Reactions Occurring During Catalytic Abatement **238**
13.3 First-Generation Converters: Oxidation Catalyst **239**
13.4 The Failure of Nonprecious Metals: A Summary of Catalyst History **240**
13.4.1 Deactivation and Stabilization of Precious Metal Oxidation Catalysts **241**
13.5 Supporting the Catalyst in the Exhaust **242**
13.5.1 Ceramic Monoliths **242**
13.5.2 Metal Monoliths **245**
13.6 Preparing the Monolith Catalyst **246**
13.7 Rate Control Regimes in Automotive Catalysts **247**
13.8 Catalyzed Monolith Nomenclature **248**
13.9 Precious Metal Recovery from Catalytic Converters **248**
13.10 Monitoring Catalytic Activity in a Monolith **248**
13.11 The Failure of the Traditional Beaded (Particulate) Catalysts for Automotive Applications **250**
13.12 NO_x, CO and HC Reduction: The Three-Way Catalyst **251**
13.13 Simulated Aging Methods **255**
13.14 Close-Coupled Catalyst **256**
13.15 Final Comments **258**
Questions **259**
Bibliography **261**

CHAPTER 14 *DIESEL ENGINE EMISSION ABATEMENT* **262**

14.1 Introduction **262**
14.1.1 Emissions from Diesel Engines **262**
14.1.2 Analytical Procedures for Particulates **264**
14.2 Catalytic Technology for Reducing Emissions from Diesel Engines **265**
14.2.1 Diesel Oxidation Catalyst **265**
14.2.2 Diesel Soot Abatement **266**
14.2.3 Controlling NO_x in Diesel Engine Exhaust **267**
Questions **272**
Bibliography **273**

CHAPTER 15 *ALTERNATIVE ENERGY SOURCES USING CATALYSIS: BIOETHANOL BY FERMENTATION, BIODIESEL BY TRANSESTERIFICATION, AND H_2-BASED FUEL CELLS* **274**

15.1 Introduction: Sources of Non-Fossil Fuel Energy **274**
15.2 Sources of Non-Fossil Fuels **276**
15.2.1 Biodiesel **276**
15.2.1.1 Production Process **276**
15.2.2 Bioethanol **277**
15.2.2.1 Process for Bioethanol from Corn **278**
15.2.3 Lignocellulose Biomass **278**

15.2.4 New Sources of Natural Gas and Oil Sands **279**
15.3 Fuel Cells **279**
15.3.1 Markets for Fuel Cells **281**
15.3.1.1 Transportation Applications **281**
15.3.1.2 Stationary Applications **282**
15.3.1.3 Portable Power Applications **282**
15.4 Types of Fuel Cells **283**
15.4.1 Low-Temperature PEM Fuel Cell **284**
15.4.1.1 Electrochemical Reactions for H_2-Fueled Systems **284**
15.4.1.2 Mechanistic Principles of the PEM Fuel Cell **286**
15.4.1.3 Membrane Electrode Assembly **287**
15.4.2 Solid Polymer Membrane **288**
15.4.3 PEM Fuel Cells Based on Direct Methanol **289**
15.4.4 Alkaline Fuel Cell **290**
15.4.5 Phosphoric Acid Fuel Cell **290**
15.4.6 Molten Carbonate Fuel Cell **291**
15.4.7 Solid Oxide Fuel Cell **293**
15.5 The Ideal Hydrogen Economy **293**
Questions **294**
Bibliography **295**

INDEX **297**

PREFACE

"Simplicity is the ultimate sophistication."

THESE WORDS of Leonardo da Vinci were recently quoted by Steve Jobs of Apple in the book by Walter Isaacson. *Simplicity* was the first guiding principle in the preparation of this introductory book. The second guiding principle was to *share our considerable industrial and academic experience* in working with and teaching about catalysis fundamentals and industrial catalytic processes.

All of us authors have worked in industry and academia, two of us as technical consultants. Dr. Farrauto was affiliated with BASF (formerly Engelhard), Iselin, New Jersey for 37 years having worked in environmental, chemical, petroleum, and alternative energy fields and is now Professor of Practice in the Earth and Environmental Engineering Department at Columbia University in the City of New York. Dr. Dorazio, a research engineer at BASF (New Jersey), has worked in catalysis research and in scale-up of catalysts for the chemical, petroleum, and environmental fields. He is also Adjunct Professor in the Chemical Engineering Department at New Jersey Institute of Technology (NJIT). Dr. Bartholomew, Professor Emeritus in the Chemical Engineering Department at Brigham Young University, Provo, Utah, worked for a year at Corning Glass (with Dr. Farrauto) in auto emissions control after which he taught and conducted research and consulting for 41 years in catalyst design/deactivation and reactor/process design for environmental cleanup and synthetic fuel production. He continues to be active in writing, teaching short courses, and consulting. All of us have been widely engaged in various degrees of teaching industrial catalysis at the undergraduate and graduate levels. Bartholomew and Farrauto have coauthored the widely used text and reference book entitled "Fundamentals of Industrial Catalytic Processes," a more advanced, in-depth version of the topics in the current book and a likely sequel to this book.

Industrial catalytic applications are seldom taught in undergraduate chemistry and chemical engineering programs, a surprising fact, given the large number of commercial processes that utilize catalysis. Thus, we accepted the challenge of writing a book that would introduce senior level undergraduates and new graduate students to this exciting field of catalytic processes, which is fundamental to chemical engineering and chemistry as practiced in industry. The need for a thorough understanding of fundamental principles of chemistry and catalysis is given. The transition of this knowledge to their commercial applications is our objective, especially for the many chemistry and chemical engineering students who spend much of their careers working in industry with catalytic processes. We also include the many professionals of varying disciplines

who suddenly find themselves with a new assignment of working on a catalytic process without previous training in the basics of catalysis and catalytic processes.

Our goal is to explain the fundamental principles of catalysis and their applications of catalysis in a simple, introductory textbook that excites those contemplating an industrial career in chemical, petroleum, alternative energy, and environmental fields in which catalytic processes play a dominant role. The book focuses on non-proprietary, basic chemistries and descriptions of important, currently used catalysts and catalytic processes. Considerable practical examples, recommendations, and cautions located throughout the book are based on authors' experience gleaned from teaching, research, commercial development, and consulting, including feedback from many students and associates. Suggested readings (reviews, books, and journal articles) are included at the end of each chapter to encourage interested readers to deepen their knowledge of these topics. Process diagrams have been simplified to provide an overview of principal process units (e.g., reactors and separation units) and important process steps, including reactant and product streams. Nevertheless, it should be recognized that commercial engineering process flow sheets include many other details and specifications, for example, piping, pumps, valves, heat exchangers, and other process equipment needed to operate and control the plant, including special equipment for plant start-up, catalyst pretreatment, purges, safety, regeneration, and so on.

Chapters 1–5 introduce the reader to basic principles of catalysis, including reaction kinetics, simple reactor design concepts, and catalyst preparation, characterization, and deactivation. Accompanying each chapter are questions and suggested readings. Chapters 6–15 describe by category applications and practice in the industry, including process chemistry, conditions, catalyst design, process design, and catalyst deactivation problems for each catalytic process. Chapter 6 describes hydrogen and syngas generation processes for different end applications. Processes for the synthesis of ammonia, methanol, and hydrocarbon liquids (Fischer–Tropsch process) are presented in Chapter 7. Processes for selective catalytic oxidation to (a) commodity chemicals, including nitric, cyanic, and sulfuric acids, formaldehyde, and ethylene oxide, and (b) specialized products such as acrylic acid, maleic anhydride, and acrylonitrile are presented in Chapter 8. Catalytic processes for hydrogenation of vegetable oils, olefins, and functional groups for highly specialized products are presented in Chapter 9. Catalytic processes in refining of petroleum to fuels are presented in Chapter 10. Selected commercial processes utilizing (a) homogeneous catalysts, (b) commercial enzymes, and (c) polymerization catalysts are described in Chapter 11. Chapters 12, 13, and 14 summarize features of important processes for catalysts used in environmental control of gaseous emissions from (a) stationary sources (e.g., power plants) and mobile sources, including (b) gasoline- and (c) diesel-fired vehicles. The final chapter 15 gives a brief summary of (1) catalytic processes for production of bio diesel and ethanol fuels from edible biomass which will ultimately find application to production of similar fuels from non-edible cellulosic biomass and (2) catalyst technology for the emerging hydrogen economy with emphasis on fuel cell technology.

New York, New York Robert J. Farrauto
Iselin, New Jersey Lucas Dorazio
Provo, Utah Calvin H. Bartholomew
22 November 2015

ACKNOWLEDGMENTS

Drs. Farrauto and Dorazio acknowledge BASF (and Engelhard) for their strong leadership in the field of catalysis. We also acknowledge our students at Columbia University and NJIT, respectively, who have provided course and teaching evaluations that have been invaluable in showing us the need for a simple approach to catalysis and industrial processes.

Dr. Bartholomew is grateful for the financial support of his research, teaching, and writing endeavors by Brigham Young University and of his research by DOE, NSF, GRI, and many companies. He wishes to acknowledge the opportunity to work with distinguished colleagues and friends on the Faculty (especially in the Chemical Engineering Department and Catalysis Laboratory) and some 200+ bright, creative, hardworking graduate and undergraduate students and postdoctoral fellows who worked with him under his direction at BYU. He has also enjoyed the stimulation of teaching more than 750 company professionals during dozens of short courses on catalysis, deactivation, and Fischer–Tropsch synthesis. He wishes to acknowledge the collaboration with and friendship of Dr. Robert Farrauto over the past 42 years, first at Corning Glass, then on a landmark paper, and now two books addressing industrial catalytic processes; he is especially grateful for Bob's patience with him during the long process of preparing the first and second editions of *Fundamentals of Industrial Catalytic Processes*.

LIST OF FIGURES

Chapter 1

Figure 1.1 Catalyzed and uncatalyzed reaction energy paths illustrating the lower energy barrier (activation energy) associated with the catalytic reaction compared with the noncatalytic reaction **2**

Figure 1.2 Illustration of catalyzed versus noncatalyzed reactions **2**

Figure 1.3 Catalytic Fe–Ce redox reaction catalyzed by Mn **3**

Figure 1.4 Activation energy diagram for (a) noncatalytic thermal reaction of CO and O_2 and (b) the same reaction in the presence of Pt. Activation energy for the noncatalyzed reaction is E_{nc}. The Pt-catalyzed reaction activation energy is designated E_c. Note that heat of reaction ΔH is the same for both reactions **4**

Figure 1.5 Conversion of CO versus temperature for a noncatalyzed (homogeneous) and catalyzed reaction **5**

Figure 1.6 Particulate catalysts for fixed bed reactors: spheres, extrudates, and tablets. Powdered catalysts for batch slurry phase processors. A cartoon of a fixed bed reactor loaded with catalyst tablets **9**

Figure 1.7 Adsorption isotherm (θ_{CO}) for CO on Pt for large, moderate, and low partial pressures of CO. The slope at low partial pressures of CO equals the adsorption equilibrium constant K_{CO} **12**

Figure 1.8 Illustration of Langmuir–Hinshelwood reaction mechanism **13**

Figure 1.9 Illustration of Mars–van Krevelen reaction mechanism **14**

Figure 1.10 Illustration of Eley–Rideal reaction mechanism **14**

Figure 1.11 L–H kinetics applied to increasing P_{CO} at constant P_{O2}. Maximum rate was achieved when an equal number of CO molecules and O atoms are adsorbed ($\theta_O = \theta_{CO}$) on adjacent Pt sites **16**

Figure 1.12 Ideal dispersion of Pt atoms on a high surface area Al_2O_3 carrier **17**

Figure 1.13 Illustration of the sequence of chemical and physical steps occurring in heterogeneous catalysis **20**

Figure 1.14 Conversion versus temperature profile illustrating regions for chemical kinetics, pore diffusion, and bulk mass transfer control **21**

Figure 1.15 Relative rates of bulk mass transfer, pore diffusion, and chemical kinetics as a function of temperature. Chemical kinetics controls the rate between temperatures *A* and *B*. Pore diffusion controls from *B* to *C* temperatures, while bulk mass transfer controls at temperatures greater than *C* **22**

Figure 1.16 Reactant concentration gradients within a spherical structured catalyst for three regimes controlling the rate of reaction **23**

Chapter 2

Figure 2.1 (a) SEM of γ-Al_2O_3 (80,000× magnification) and (b) SEM of α-Al_2O_3 (80,000× magnification) **33**

Figure 2.2 Three zeolites: (a) mordenite, (b) ZSM-5, and (c) Beta **36**

Figure 2.3 Ceramic and metallic (center image) monoliths of different shapes and cell geometries **41**

Figure 2.4 Ceramic washcoated monoliths **44**

Chapter 3

Figure 3.1 (a) Adsorption isotherm for nitrogen for BET surface area measurement. (b) Linear plot of the BET equation for surface area measurement. (c) Nitrogen adsorption/desorption isotherm for pore size measurement **50**

Figure 3.2 Mercury penetration as a function of pore size of catalyst **52**

Figure 3.3 Differential porosimetry for a porous catalyst **52**

Figure 3.4 Particle size measurement using laser light scattering analysis **53**

Figure 3.5 Thermal gravimetric analysis and differential thermal analysis of the decomposition of barium acetate on ceria **55**

Figure 3.6 Electron microprobe showing a two-washcoat-layer monolith catalyst. The top layer is Rh on Al_2O_3 and the bottom layer is Pt on Al_2O_3 **57**

Figure 3.7 SEM of γ-Al_2O_3 with its highly porous network **58**

Figure 3.8 X-ray diffraction patterns of γ- and α-Al_2O_3 **59**

Figure 3.9 (a) Chemisorption isotherm for determining surface area of the catalytic component. (b) Pulse chemisorption profiles for the dynamic chemisorption method **60**

Figure 3.10 Transmission electron micrograph of Pt on TiO_2 **61**

Figure 3.11 Transmission electron micrograph of Pt on CeO_2 **62**

Figure 3.12 X-ray diffraction profile for different crystallite sizes of CeO_2 **63**

Figure 3.13 An XPS spectrum of various oxidation states of palladium on Al_2O_3 **64**

Figure 3.14 NMR profile of a Y faujasite zeolite **65**

Figure 3.15 DRIFT spectra of CO chemisorbed on different precious metal particles of catalysts prepared in different ways. The CO chemisorption followed by FT-IR measurements was performed at room temperature after the catalysts were treated at 400 °C for 1 h with 7% H_2 in Ar gas **66**

Chapter 4

Figure 4.1 Illustration of the three processes that can limit the reaction rate during heterogeneous catalysis **70**

Figure 4.2 Illustration showing how experimental rate measurements can be plotted in order to determine the concentration dependence used in the power rate law **74**

Figure 4.3 Illustration showing how experimental rate measurements can be plotted in order to determine the activation energy and pre-exponential factor used in the Arrhenius expression **75**

Figure 4.4 Conversion versus temperature at different space velocities. Experiment is performed to determine the rate constant at various temperatures **76**

Figure 4.5 Arrhenius plot for determining activation energies **83**

Chapter 5

Figure 5.1 Idealized cartoon of perfectly dispersed Pt on a high-surface γ-Al_2O_3 **89**

Figure 5.2 Conceptual diagram of sintering of the catalytic component on a carrier **90**

Figure 5.3 TEM of fresh and sintered Pt on Al_2O_3 in an automobile catalytic converter application. "Black dots" are platinum crystallites. The size difference in crystallites between the two pictures is the result of sintering **90**

Figure 5.4 Idealized conversion versus temperature for various aging phenomena **91**

Figure 5.5 Illustration of the sintering of the catalyst carrier occluding the catalytic component **92**

Figure 5.6 Microscopy images of low surface area rutile (a) and high surface area anatase (b). Each set of four photos show the structure at increasing magnification **93**

Figure 5.7 (a) NMR profile of a thermally aged zeolite showing the loss of the Si–O–Al bridges. Si(3Al), Si(2Al), and Si(Al) are seen to decrease in intensity with the progressively more severe thermal aging. (b) Growth of penta- and octahedral coordination sites in a thermally deactivated zeolite **94**

Figure 5.8 Conceptual cartoon showing selective poisoning of the catalytic sites **96**

Figure 5.9 Conceptual cartoon showing masking or fouling of a catalyst washcoat **97**

Figure 5.10 XPS spectrum of the surface of a contaminated Pt on Al_2O_3 catalyst **98**

Figure 5.11 Electron microprobe showing the deposition location of the poisons within the washcoat of a monolith catalyst used in an automobile catalytic converter. The X-ray beam is scanned perpendicular to the axial direction through thickness of the washcoat **98**

Figure 5.12 TGA/DTA in air of coke burn-off from a catalyst **100**

Figure 5.13 TGA/DTA profile for desulfation of Pd on Al_2O_3 catalyst **100**

Chapter 6

Figure 6.1 Illustration of industrial hydrogen generation process **105**

Figure 6.2 A series of metallic tubes filled with particulate catalysts bathed in a furnace of burning natural gas providing the required heat of reaction. The rate of reaction and temperature are highest near the heat source **108**

Figure 6.3 Reduction or activation of Ni SR catalyst: H_2O (steam)/H_2 as a function of temperature for redox of NiO/Ni **109**

Figure 6.4 H_2O/C versus temperature: a high H_2O/CH_4 ratio allows higher temperatures for coke-free operation. To the right of the line is the coke forming regime **110**

Figure 6.5 WGS equilibrium: free energy and equilibrium constant for WGS as a function of temperature **114**

Figure 6.6 Typical performance of a HTS WGS catalyst with respect to exit CO **115**

Figure 6.7 Reformer schematic for pure H_2 **118**

Figure 6.8 Overall process flow diagram for preformed natural gas to H_2 and N_2 for NH_3 production **119**

Figure 6.9 Monolith catalysts for H_2 generation using PSA or PROX **123**

Figure 6.10 Illustration of a highly simplified catalyzed double pipe heat exchanger where a combustion catalyst is applied to the inside surface and a steam reforming catalyst is applied to the outside surface of the inner tube **124**

Figure 6.11 Preferential oxidation of 0.5% CO using a (Pt, Fe, Cu)/Al_2O_3 monolith catalyst **125**

Figure 6.12 Various catalytic processes for generating H_2 and synthesis gas from desulfurized natural gas (methane) and methanol **127**

Chapter 7

Figure 7.1 Simplified flow sheet for NH_3 synthesis illustrating a "quench"-type ammonia converter and two-stage feed gas compression **130**

Figure 7.2 Simplified illustration of a single-stage radial flow ammonia converter **134**

Figure 7.3 Illustration of methanol quench reactor design **136**

Figure 7.4 Illustration of staged cooling design **137**

Figure 7.5 Illustration of cooled tube reactor design **138**

Figure 7.6 Illustration of shell-cooled reactor design **138**

Figure 7.7 Flow sheet for methanol synthesis **139**

Figure 7.8 Bubble slurry reactor for Fischer–Tropsch **142**

Figure 7.9 Loop reactor for Fischer–Tropsch **144**

Chapter 8

Figure 8.1 Surface roughening (sprouting of PtRh gauze) **148**

Figure 8.2 High-pressure NH_3 oxidation/HNO_3 plant with Pd getter gauze **149**

Figure 8.3 An expanded view of the reactor containing the stacks of oxidation and getter gauzes **150**

Figure 8.4 HCN process flow diagram **153**

Figure 8.5 The Claus process with staged reaction and liquid sulfur removal **154**

Figure 8.6 Elemental sulfur is reacted with dry air at 900 °C producing SO_2. Staged air injection into the second and third stages for cooling is shown in Figure 8.8 **156**

Figure 8.7 SO_2/SO_3 equilibrium as a function of temperature **157**

Figure 8.8 Quench reactor for SO_3 production with staged air injection for cooling for stages 2 and 3 **158**

Figure 8.9 The O_2 process for ethylene oxide production **161**

Figure 8.10 Process for low methanol concentration process to formaldehyde over a (Fe, Mo)/SiO_2 catalyst **162**

Figure 8.11 Process using Ag catalyst **163**

Figure 8.12 Propylene to acrolein to acrylic acid process flow diagram. Tubular reactor with a diameter of about 2.5 cm and a length of about 4 m cooled by a molten carbonate **165**

Figure 8.13 Process for converting propylene to acrylonitrile **167**

Chapter 9

Figure 9.1 Illustration comparing difference between a semibatch stirred tank reactor and a continuous stirred tank reactor **172**

Figure 9.2 Illustration of a semibatch stirred tank reactor (STR). The sparger (or also called dip tube) is used for continuous addition of a reactant, which is hydrogen for hydrogenation reactions. Not shown is the removal of unreacted hydrogen from the headspace, which must occur to maintain the desired reactor pressure **173**

Figure 9.3 Illustration showing hydrogen consumption versus time during typical hydrogenation reaction **173**

Figure 9.4 Illustration of the mass transfer path taken by hydrogen as it diffuses from the gas bubble, through the bulk liquid, and ultimately to the catalyst particle. In most hydrogenation reactions, the rate of this diffusion process limits the overall rate of reaction **174**

Figure 9.5 Kinetic rate for a catalytic slurry-phase batch reaction **176**

Figure 9.6 Linolenic oil shown as an example of an unsaturated fat molecule **178**

Figure 9.7 Sequential reactions at 140 and 200 °C **179**

Figure 9.8 CATOFIN propane dehydrogenation to propylene using Cr_2O_3/Al_2O_3 catalyst **185**

Figure 9.9 Flow diagram for dehydrogenation of ethyl benzene to styrene **187**

Chapter 10

Figure 10.1 Simplified illustration of the crude oil refining process. The desalting process (removal of inorganic components in the crude using a water wash) is not shown **192**

Figure 10.2 Examples of metal-containing (nickel porphyrin) and sulfur-containing (thiophene) species typically found in crude oil **193**

Figure 10.3 The HDM/HDS process flow diagram. Inset shows presulfided catalyst and its positive effect on decreasing excessive gas make and hydrogen consumption **195**

Figure 10.4 Catalyst deactivation by HDM metal deposition (masking) and coking **196**

Figure 10.5 Controlled O_2 addition in coked catalyst regeneration **196**

Figure 10.6 Faujasite zeolite **198**

Figure 10.7 Schematic of FCC reactor with catalyst regenerator **199**

Figure 10.8 Process flow diagram for naphtha reforming **201**

Figure 10.9 Regeneration and rejuvenation of (Pt, Re)/γ-$Al_2O_3 + Cl^-$ reforming catalyst **202**

Chapter 11

Figure 11.1 Hydroformylation process using a cobalt homogeneous catalyst **207**

Figure 11.2 Dow (Davy McKee) LP Oxo Selector process using the Rh catalyst **207**

Figure 11.3 Monsanto acetic acid process **209**

Figure 11.4 Phillips loop reactor **211**

Figure 11.5 $TiCl_3/MgCl_2$ process for polyethylene **212**

Chapter 12

Figure 12.1 (a) VOC abatement process with heat integration. (b) VOC abatement with supplemental heating **223**

Figure 12.2 Slipstream reactor concept used for VOC abatement design **224**

Figure 12.3 Catalyst abatement of food processing fumes **225**

Figure 12.4 SCR with V_2O_5 and a metal-exchanged zeolite: 1.1 NH_3/NO and zeolite **228**

Figure 12.5 SCR reactor schematic. It would be worth mentioning that the widening, that is, lower velocity, increases contact time **229**

Figure 12.6 Ozone abatement reactor design **230**

Chapter 13

Figure 13.1 Gasoline-relative engine emissions and temperature as a function of air/fuel ratio **236**

Figure 13.2 Monolith catalyst housed in a metal canister secured in the exhaust **239**

Figure 13.3 Optical micrographs of double-layered washcoated ceramic monoliths **243**

Figure 13.4 Conversion proceeding axially down the channel of a monolith with poisoning. Units of time are arbitrary units **249**

Figure 13.5 Temperature profiles ($\Delta T/\Delta L$) for an exothermic reaction down the axial length of a catalyzed monolith channel caused by sintering **250**

Figure 13.6 Simultaneous conversion of HC, CO, and NO_x for TWC as a function of air/fuel ratio **252**

Figure 13.7 Oxygen sensor response output as a function of air/fuel ratio **253**

Figure 13.8 Electron microprobe scan of an automotive catalyst contaminated with P and S from lubricating oil **255**

Figure 13.9 Close-coupled TWC catalyst, under-floor TWC, and oxygen sensors connected to electronic feedback to control air/fuel ratio close to stoichiometric ($\lambda = 1$) **258**

Chapter 14

Figure 14.1 NO_x–particulate trade-off with emission regulations **263**

Figure 14.2 Electron microprobe scans of the washcoat of an aged diesel oxidation catalyst. (a) Zn and Ca. (b) P and S **266**

Figure 14.3 Wall flow filter. Soot particulates deposit on the porous wall, while the gaseous components (CO_2, H_2O, NO, and NO_2) and air pass through. The soot is combusted periodically by raising the inlet temperature to >500 °C when a small amount of diesel fuel is injected into the DOC **267**

Figure 14.4 SCR with Cu and Fe zeolites **268**

Figure 14.5 Schematic of simplified diesel exhaust aftertreatment system. A diesel oxidation catalyst and wall flow filter (or diesel particulate filter) are contained in one canister, a dosing system for injecting urea to the SCR catalyst. An ammonia decomposition catalyst (Pt/γ-Al_2O_3//ceramic monolith) is installed at the outlet of SCR. The DOC catalyzes the oxidation of CO, HC, and some of the NO to NO_2 and generates sufficient heat (~500 °C) by oxidizing injected diesel fuel to initiate combustion of the soot collected on

the wall flow filter. The NO and NO_2 exiting the filter are mixed with inject urea, which hydrolyzes to NH_3 and enters the SCR catalyst. EGR may be used to further reduce the engine out NO. Not shown is a turbocharger than compresses the air as it enters the combustion chamber. This further enhances the power of the engine to move heavy loads **269**

Figure 14.6 Chemistry of NO_x reduction in using BaO to capture NO_2 during lean operation **270**

Figure 14.7 Deactivation of the NO_x trap by sulfur oxide poisoning **271**

Figure 14.8 Driving profile for a LNT. During lean mode (fuel economy), NO is converted to NO_2 over a Pt catalyst, which is adsorbed in the alkaline trap. Regeneration (solid area) occurs when the engine is commanded to a stoichiometric mode where the NO_x is desorbed from the BaO and the Rh in the TWC reduces it to N_2 **271**

Chapter 15

Figure 15.1 Biodiesel production process **277**

Figure 15.2 A comparison of power generation for a coal-fired power plant, gasoline/diesel internal combustion engine, and a H_2–O_2 low-temperature fuel cell **280**

Figure 15.3 A single cell of the PEM fuel cell **285**

Figure 15.4 Voltage–current profile for the PEM fuel cell. The curve with the maxima represents the power profile **286**

Figure 15.5 A PEM single cell and arranged in a "stack." Each cell is separated by an electrically conductive impermeable bipolar plate that serves as a gas manifold for the cells connected in series **288**

Figure 15.6 Ideal H_2 economy with the sun providing energy for a photovoltaic device generating sufficient voltage to electrolyze water to H_2 and O_2 **294**

NOMENCLATURE

SYMBOLS

A	Frontal area (m^2)
a_s	Geometric surface area = ratio of surface area to volume (m^{-1})
a_{Sh}	Fitted parameter used for mass transfer coefficient
B	Integral breadth (Scherrer's formula) (°)
C	Concentration (mol/m^3)
C_{BET}	BET constant
C_{WP}	Weisz–Prater criterion
D	Diffusivity (m^2/s)
D_e	Effective diffusivity (m^2/s)
D_k	Knudsen diffusivity (m^2/s)
d_p	Particle diameter (d_h) = monolith channel diameter (m)
d_{pore}	Pore diameter (m)
E_A	Activation energy (J/mol)
E_{cell}	Net voltage of fuel cell (V)
E°_{cell}	Standard state cell voltage (V)
E_o	Standard state voltage in the Nernst equation (V)
f	Friction factor
F	Molar flow (mol/s)
F_c	Faraday constant (C/V)
g_c	Gravitational constant (m/s^2)
GHSV	Gas hourly space velocity (h^{-1})
ΔG_{rxn}	Free energy change during reaction (J/mol)
H	Henry's law constant
ΔH_{rxn}	Enthalpy change during reaction (J/mol)
J	Molar flux ($mol/(m^2\ s)$)
k	Reaction rate constant (mol/(s l))
K_{eq}	Equilibrium constant
k_f, k_d	Rate constants for absorption and desorption (mol/(s l))
k_{MT}	Mass transfer coefficient (m/s)
k_o	Pre-exponential factor (g)
M_{flow}	Mass flow rate (kg/h)
MW	Molecular weight (mol/g)
n	Number of electrons transferred
N_A	Avogadro's number (mol^{-1})
P	Pressure (atm)
P_i	Partial pressure of species i (atm)

P_o	Saturation pressure (atm)
r	Reaction rate per unit volume (mol/(s l))
r'	Reaction rate per unit mass (mol/(s g))
R	Ideal gas constant (J/(mol K))
Re	Reynolds number
r_k	Rate of reaction on catalyst surface (mol/(s l))
r_{MT}	Rate of bulk diffusion (mol/(s l))
$r_{MT,g}$	Rate of bulk diffusion through gas phase (mol/(s l))
$r_{MT,g-l}$	Rate of diffusion through gas–liquid interface (mol/(s l))
$r_{MT,l-s}$	Rate of diffusion through liquid–solid interface (mol/(s l))
r_p	Pore radius (m)
R_{pellet}	Radius of catalyst pellet (m)
r_{pore}	Rate of pore diffusion (mol/(s g))
Sc	Schmidt number
Sh	Sherwood number
ΔS_{rxn}	Entropy change during reaction (J/K)
SV	Space velocity (h^{-1})
t	Residence time (min or h)
T	Temperature (°C or K)
t_{crys}	Thickness of crystallite (Scherrer's formula) (nm)
u	Bulk stream velocity (m/s)
V	Reactor volume (m^3)
V_{ad}	Volume adsorbed at P (m^3)
V_{flow}	Volumetric flow (m^3/s)
V_m	Molar volume (mol/m^3)
V_{mono}	Adsorbed volume at monolayer coverage (m^3)
v_o	Volumetric flow rate (m^3/h)
V_{rxtr}	Reactor volume (m^3)
W_{cat}	Catalyst mass (g)
WHSV	Weight hourly space velocity (h^{-1})
X	Fractional conversion
x_{Sh}	Fitted parameter used for mass transfer coefficient
Z	Reactor length (m)

GREEK SYMBOLS

β	Approach to equilibrium
γ	Surface tension (N/m)
δ_M	Thickness of mass transfer boundary layer (m)
ε	Binary interaction energy (K)
ε	Void fraction in the bed
ε_p	Particle porosity
θ	Contact angle (°)
θ_d	Bragg angle (°)